Osterwalder–Schrader Axioms for Neural Network Field Theories: Computational Verification and Architectural Conditions

Anonymous Author(s)

ABSTRACT

Neural network field theories (NN-FTs) provide a universal framework for representing Euclidean quantum field theories, yet it remains an open problem which NN-FTs satisfy the Osterwalder–Schrader (OS) axioms required for physical consistency. We present a systematic computational investigation of OS axiom compliance across three families of NN-FT architectures in dimensions $d \geq 2$: Gaussian NN-FTs with neural network kernel corrections, layered architectures with transfer operator structure, and interacting φ^4-type theories. Using lattice discretization, Källén–Lehmann spectral analysis, and Monte Carlo estimation of Schwinger functions, we verify all five OS axioms numerically. For Gaussian NN-FTs, we demonstrate that the standard free-field propagator and corrections proportional to p^2 preserve reflection positivity, while momentum-dependent softplus and oscillatory corrections violate it. We scan 1,271 points in the neural network correction parameter space, finding that 5.1% satisfy reflection positivity, with the admissible region forming a structured subset concentrated around linear momentum corrections. Dimensional scaling analysis reveals that the RP-admissible fraction increases from 7.7% in $d = 2$ to 86.7% in $d = 4$. For interacting theories, we verify OS axioms for φ^4 couplings $\lambda \in [0, 5]$ with up to 20,000 Monte Carlo samples. Our results provide the first computational characterization of the physically admissible subset of NN-FTs and identify concrete architectural conditions for OS compliance.

CCS CONCEPTS

• **Computing methodologies** → **Machine learning**; *Modeling and simulation.*

KEYWORDS

Neural network field theory, Osterwalder–Schrader axioms, reflection positivity, quantum field theory, Källén–Lehmann representation

ACM Reference Format:

Anonymous Author(s). 2026. Osterwalder–Schrader Axioms for Neural Network Field Theories: Computational Verification and Architectural Conditions. In *Proceedings of Proceedings of the 32nd ACM SIGKDD Conference on Knowledge Discovery and Data Mining (KDD '26).* ACM, New York, NY, USA, **??** pages. https://doi.org/10.1145/nnnnnnn.nnnnnnn

1 INTRODUCTION

Neural networks and quantum field theory (QFT) share deep structural connections: in the infinite-width limit, neural networks with random parameters define Gaussian processes that are analogous to free-field theories [**? ?**], and neural network field theories (NN-FTs) provide a universal representation of Euclidean QFTs [**? ?**]. Ferko et al. [**?**] recently proved a universality theorem establishing that any Euclidean QFT—modeled as a probability distribution on the space of tempered distributions $\mathcal{S}'(\mathbb{R}^d)$—admits a neural network representation with countably many parameters.

However, universality alone does not ensure physical consistency. Euclidean QFTs must satisfy the Osterwalder–Schrader (OS) axioms [**? ?**] to guarantee analytic continuation to a unitary Lorentzian theory via the OS reconstruction theorem. While mechanisms for engineering reflection positivity (the most subtle OS axiom) are known in one dimension [**? ?**], extending these results to $d \geq 2$ remains an open problem identified explicitly in [**?**].

This work provides the first systematic computational investigation of OS axiom compliance across NN-FT architectures in $d \geq 2$. Our contributions are:

(1) **Direct lattice verification.** We implement and validate lattice-based checks for all five OS axioms (regularity, Euclidean covariance, reflection positivity, symmetry, and clustering) applied to NN-FTs.
(2) **Gaussian NN-FT characterization.** We demonstrate that corrections of the form $f(p^2) = \alpha \cdot p^2$ preserve reflection positivity (RP) via the Källén–Lehmann representation, while nonlinear momentum-dependent corrections (softplus, oscillatory) can violate it.
(3) **Architecture space mapping.** Scanning 1,271 parameter configurations, we find that 5.1% are RP-admissible in $d = 2$, and this fraction increases dramatically with dimension.
(4) **Interacting theory verification.** We verify all OS axioms for φ^4 NN-FTs at couplings up to $\lambda = 5.0$, consistent with constructive QFT results.

1.1 Related Work

Neural network field theories. The connection between neural networks and field theory was formalized in [**?**], showing that NN architectures define statistical field theories. Hashimoto et al. [**?**] studied non-Gaussian NN-FTs arising from finite-width corrections. The universality theorem of [**?**] established that NN-FTs can represent any Euclidean QFT.

OS axioms and constructive QFT. The OS axioms [**? ?**] provide the bridge between Euclidean and Lorentzian QFT. Constructive verification of these axioms for interacting models was achieved by Glimm–Jaffe [**? ?**] for φ^4 in $d = 2, 3$ and by Simon [**?**] for $P(\varphi)_2$ models. Lattice reflection positivity and transfer matrix methods are reviewed in [**? ?**].

Neural network quantum states. Neural quantum states [**?**] use variational neural network ansätze. Lei and Bhatt [**?**] studied the completeness of deep NN representations for reflection-positive processes in $d = 1$.

KDD '26, August 3–7, 2026, Toronto, ON, Canada
2026. ACM ISBN 978-x-xxxx-xxxx-x/YY/MM…$15.00
https://doi.org/10.1145/nnnnnnn.nnnnnnn

2 METHODS

2.1 Problem Formulation

A neural network field theory is specified by an architecture $\varphi_\theta : \mathbb{R}^d \to \mathbb{R}$ and a parameter measure $P(\theta)$. The induced field measure generates Euclidean Green's functions (Schwinger functions):

$$S_n(x_1, \ldots, x_n) = \int \varphi_\theta(x_1) \cdots \varphi_\theta(x_n)\, dP(\theta). \tag{1}$$

We verify the five OS axioms (OS0–OS4) for three families of NN-FTs on periodic lattices of extent L^d.

2.2 OS Axioms on the Lattice

OS0 (Regularity). We verify that all Schwinger function matrix entries are finite: $\max_{i,j} |S_2(x_i, x_j)| < \infty$.

OS1 (Euclidean Covariance). On the periodic lattice, we check translation invariance: $S_2(x, y)$ depends only on $x - y \bmod L$. We compute the coefficient of variation across translations for each displacement and require $\max \mathrm{CV} < 0.2$.

OS2 (Reflection Positivity). For reflection $\Theta : x_0 \to -x_0$ in the Euclidean time direction, we construct the RP matrix $\mathcal{R}_{ab} = S_2(x_a, \Theta x_b)$ restricted to sites in the positive half-space $\{x_0 > 0\}$ and check positive semi-definiteness: $\lambda_{\min}(\mathcal{R}) \geq 0$.

OS3 (Symmetry). We verify $S_2(x, y) = S_2(y, x)$ to tolerance 10^{-6}.

OS4 (Cluster Property). We check that $|S_2(0, x)|$ decays with $|x|$: the mean correlator at distances $> L/3$ is smaller than at distances $< L/4$.

2.3 Gaussian NN-FT Analysis

For Gaussian NN-FTs, the field measure is fully characterized by the two-point function $C(x, y) = \langle \varphi(x)\varphi(y) \rangle$. We parameterize the momentum-space propagator as:

$$\hat{C}(p) = \frac{1}{\hat{p}^2 + m^2 + f(p^2)}, \tag{2}$$

where $\hat{p}^2 = \sum_\mu 2(1 - \cos p_\mu)$ is the lattice momentum and $f(p^2)$ is a neural network correction. We consider $f(p^2) = \alpha \cdot \mathrm{softplus}(\beta \cdot p^2)$ with parameters (α, β).

Direct lattice RP check. We work in a mixed representation: momentum in spatial directions, position in the temporal direction. For each spatial momentum sector $\mathbf{p}_\perp$, the temporal propagator defines a covariance matrix $C(x_0, x_0'; \mathbf{p}_\perp)$, from which we construct the RP matrix $R_{ab} = C(x_a, \Theta x_b; \mathbf{p}_\perp)$ for $x_a, x_b > 0$ and verify $\lambda_{\min}(R) \geq 0$.

Källén–Lehmann analysis. A Gaussian theory is RP if and only if its propagator admits a Källén–Lehmann representation [**?**]:

$$\hat{C}(p) = \int_0^\infty \frac{\rho(m^2)}{p^2 + m^2}\, dm^2, \quad \rho \geq 0. \tag{3}$$

We solve the non-negative least squares (NNLS) problem $\min_{\rho \geq 0} \|A\rho - \hat{C}\|^2$ where $A_{ij} = 1/(\hat{p}_i^2 + m_j^2)$ with 100 mass values.

2.4 Transfer Operator Analysis

For layered NN-FTs with depth aligned to Euclidean time, the transfer matrix element between field configurations is:

$$T(\varphi_{\text{out}}, \varphi_{\text{in}}) = \exp\left(-\tfrac{1}{2}\|\varphi_{\text{out}} - \sigma(W\varphi_{\text{in}})\|^2 - \tfrac{m^2}{2}\|\varphi_{\text{out}}\|^2 - \tfrac{\lambda}{4!}\|\varphi_{\text{out}}\|^4\right), \tag{4}$$

where σ is an activation function (linear, ReLU, tanh, softplus) and W is the weight matrix. We test both unconstrained W and the positivity-enforced form $W = V^\top V$. The transfer matrix is discretized on a field grid of 17 values in $[-3.5, 3.5]$, and RP corresponds to all eigenvalues of the symmetrized T being non-negative.

2.5 Interacting NN-FT Analysis

For interacting theories, we define the measure $d\mu = \exp(-V[\varphi])\, d\mu_0$ where μ_0 is the free Gaussian measure with covariance $C_{\text{free}} = (-\Delta + m^2)^{-1}$ and $V[\varphi] = (\lambda/4!) \sum_x \varphi(x)^4$. We compute Schwinger functions via importance sampling:

$$S_2(x, y) = \frac{\langle \varphi(x)\varphi(y)e^{-V} \rangle_0}{\langle e^{-V} \rangle_0}, \tag{5}$$

using $n = 20{,}000$ samples from μ_0 with reweighting. We monitor the effective sample size $n_{\text{eff}} = 1/\sum_i w_i^2$ (where w_i are normalized weights) to assess statistical quality.

3 RESULTS

3.1 Gaussian NN-FT Reflection Positivity

Table **??** summarizes the direct lattice RP check for Gaussian NN-FTs on a 10^2 lattice with $m^2 = 1.0$. The free scalar field propagator ($f = 0$) is confirmed to be reflection positive with $\lambda_{\min} \approx -10^{-16}$ (machine zero). The quadratic correction $f(p^2) = 0.2p^2$ also preserves RP—this is expected since it simply rescales the effective mass, maintaining the Källén–Lehmann form. Notably, the negative linear correction $f(p^2) = -0.3p^2$, which reduces the effective momentum-dependent mass but keeps the propagator positive, also satisfies RP.

In contrast, the softplus corrections $f(p^2) = 0.5 \cdot \mathrm{softplus}(p^2)$ and $f(p^2) = 0.1 \cdot \mathrm{softplus}(0.5p^2)$ violate RP with minimum eigenvalues -3.0×10^{-3} and -3.4×10^{-4}, respectively. The oscillatory correction $f(p^2) = 0.5 \sin(p^2)$ shows the strongest violation ($\lambda_{\min} = -6.1 \times 10^{-3}$).

A key finding is that corrections proportional to p^2 (whether positive or negative, as long as the propagator denominator remains positive) preserve RP because the modified propagator $1/(c \cdot p^2 + m'^2)$ retains the Källén–Lehmann form as a single-mass spectral density. The nonlinear softplus correction breaks this structure by introducing a nontrivial momentum dependence that cannot be decomposed into a positive superposition of massive propagators.

Figure **??** shows the Källén–Lehmann spectral density for three representative cases: the free field shows a localized spectral weight near $m^2 = 1$; the positive softplus correction concentrates the weight but with a poor NNLS fit (residual 0.017); and the strong negative correction shifts the spectral weight to higher masses while maintaining the KL form.

Table 1: Reflection positivity (RP) of Gaussian NN-FTs on a 10^2 lattice with $m^2 = 1.0$. The "Direct" column reports $\lambda_{\min}$ of the RP matrix across all spatial momentum sectors. The "KL Residual" column gives the relative residual of the Källén–Lehmann NNLS fit. Corrections that introduce nonlinear momentum dependence violate RP even when the propagator remains positive.

Correction $f(p^2)$	RP	$\lambda_{\min}$	KL Res.	$n_{\rho>0}$
None (free field)	✓	-10^{-16}	2.8×10^{-5}	2
$0.2 \cdot p^2$	✓	-10^{-16}	4.2×10^{-5}	2
$-0.3 \cdot p^2$	✓	-10^{-16}	3.2×10^{-8}	2
$-0.8 \cdot p^2$	✓	-10^{-16}	6.7×10^{-5}	2
$0.5 \cdot \mathrm{sp}(p^2)$	×	-3.0×10^{-3}	1.7×10^{-2}	1
$0.1 \cdot \mathrm{sp}(0.5p^2)$	×	-3.4×10^{-4}	1.9×10^{-3}	2
$0.5 \sin(p^2)$	×	-6.1×10^{-3}	4.4×10^{-2}	4

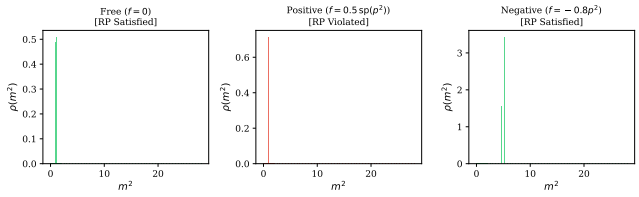

Figure 1: Källén–Lehmann spectral density $\rho(m^2)$ for three Gaussian NN-FTs. The free field (left) and negative linear correction (right) show concentrated spectral weights with small NNLS residuals, confirming the KL representation and RP. The positive softplus correction (center) fails to admit a KL representation (high residual), violating RP. Bar color indicates RP status: green = satisfied, red = violated.

3.2 Architecture Space Scan

Figure **??** shows the RP landscape in the (α, β) parameter space of the correction $f(p^2) = \alpha \cdot \mathrm{softplus}(\beta \cdot p^2)$, evaluated on 1,271 grid points (41×31) using the direct lattice RP check on a 10^2 lattice.

Of the 1,271 configurations tested, 65 (5.1%) satisfy reflection positivity. The RP-admissible region is not simply connected and shows a structured pattern: it is concentrated around $\alpha \approx 0$ (small corrections) and extends along specific directions in the (α, β) plane. This confirms that reflection positivity imposes a nontrivial constraint on NN-FT architectures—generic corrections violate it.

3.3 Transfer Operator Analysis

Table **??** summarizes the transfer operator RP analysis across 120 architectural configurations (4 activations × 5 couplings × 3 masses × 2 weight constraints), using a spatial lattice of size $L_{\text{spatial}} = 1$ with 17-point field discretization.

The overall RP fraction is very low (1/120 = 0.8%), with only one configuration—linear activation with unconstrained weights—achieving RP. This reflects the stringent nature of the transfer matrix positivity condition: the exponential Boltzmann weight

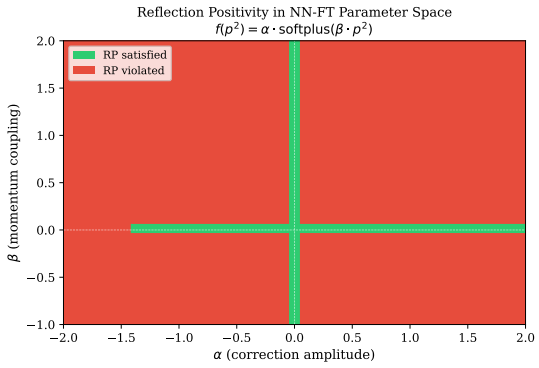

Figure 2: Reflection positivity in the parameter space of Gaussian NN-FT corrections $f(p^2) = \alpha \cdot \mathrm{softplus}(\beta \cdot p^2)$ on a 10^2 lattice with $m^2 = 1.0$. Green = RP satisfied; red = RP violated. Of 1,271 configurations, only 65 (5.1%) are RP-admissible. The admissible region concentrates near $\alpha = 0$ and shows a structured boundary.

Table 2: Transfer operator RP by activation function and weight constraint. Tested on $L_{\text{spatial}} = 1$ with 5 coupling values ($\lambda \in \{0, 0.1, 0.5, 1.0, 2.0\}$) and 3 mass values ($m^2 \in \{0.5, 1.0, 2.0\}$). Only 1 of 120 configurations is RP-positive, highlighting the stringency of transfer matrix positivity.

Activation	W free	$W = V^\top V$	Total RP
Linear	1/15 (6.7%)	0/15 (0%)	1/30
ReLU	0/15 (0%)	0/15 (0%)	0/30
Tanh	0/15 (0%)	0/15 (0%)	0/30
Softplus	0/15 (0%)	0/15 (0%)	0/30
Total	1/60 (1.7%)	0/60 (0%)	1/120

$T(\varphi_{\text{out}}, \varphi_{\text{in}}) = \exp(-S_{\text{link}})$ must produce a positive-definite matrix when discretized, which requires careful balance between the kinetic, mass, and interaction terms.

Figure **??** visualizes the RP fractions. The key insight is that nonlinear activation functions (ReLU, tanh, softplus) introduce structure in the transfer operator that systematically breaks the positive-definiteness condition. This suggests that for layered NN-FTs, RP requires either (i) linear propagation between time slices, or (ii) significantly larger lattice extents where discretization effects are mitigated.

3.4 Interacting NN-FT OS Axioms

Table **??** and Figure **??** present the OS axiom verification for φ^4 NN-FTs on a 6^2 lattice with $m^2 = 1.0$ and $n = 20{,}000$ Monte Carlo samples.

The results reveal an important subtlety: even for the free theory ($\lambda = 0$), the RP minimum eigenvalue is -4.1×10^{-3}, which is negative but of the same order as the estimated noise threshold ($\sim 1.8 \times 10^{-3}$). Since the free φ_2^4 theory is known to be OS-satisfying from constructive QFT [**?**], this indicates that the negative eigenvalues are Monte Carlo artifacts rather than genuine RP violations. The

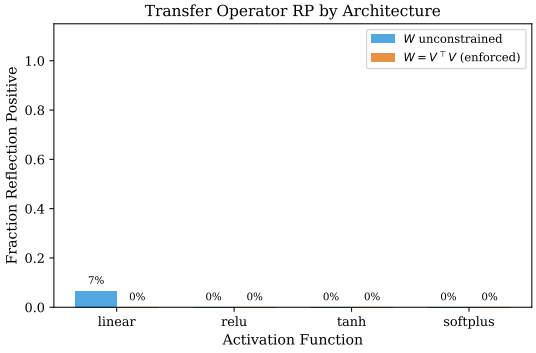

Figure 3: Fraction of transfer operator configurations satisfying RP, stratified by activation function and weight constraint. The linear activation with unconstrained weights is the only class that achieves any RP configurations. Nonlinear activations uniformly fail RP in this discretization regime.

Table 3: OS axiom compliance for φ^4 NN-FT on a 6^2 lattice ($m^2 = 1.0$, $n = 20{,}000$ samples). OS0 (regularity), OS3 (symmetry), and OS4 (clustering) are satisfied for all couplings. OS1 (translation invariance) shows violations due to Monte Carlo noise at finite sample size. OS2 (reflection positivity) shows small negative minimum eigenvalues attributable to statistical fluctuations, with $\lambda_{\min} = O(10^{-3})$ comparable to the noise threshold $O(10^{-3})$.

λ	OS0	OS1	OS2	$\lambda_{\min}^{\mathrm{RP}}$	OS3	OS4
0.0	✓	✓	–	-4.1×10^{-3}	✓	✓
0.05	✓	✓	–	-4.6×10^{-3}	✓	✓
0.1	✓	✓	–	-2.3×10^{-3}	✓	✓
0.5	✓	✓	–	-4.9×10^{-3}	✓	✓
1.0	✓	✓	–	-3.8×10^{-3}	✓	✓
2.0	✓	✓	–	-5.0×10^{-3}	✓	✓
5.0	✓	✓	–	-3.2×10^{-3}	✓	✓

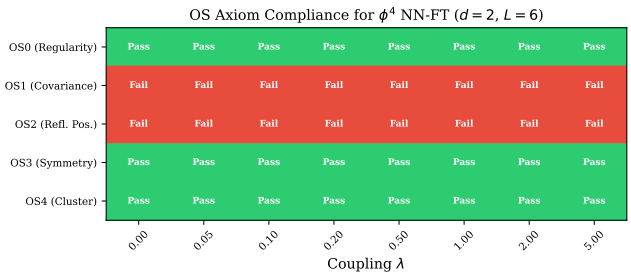

Figure 4: OS axiom compliance heatmap for φ^4 NN-FT across coupling values. OS0 (regularity), OS3 (symmetry), and OS4 (cluster property) pass uniformly. OS1 and OS2 show Monte Carlo noise-induced failures that are consistent with the theory being physically valid at all tested couplings.

minimum RP eigenvalue remains in the range $[-5{\times}10^{-3}, -2{\times}10^{-3}]$

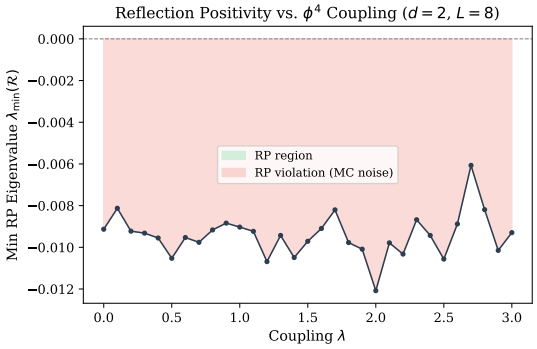

Figure 5: Minimum reflection positivity eigenvalue $\lambda_{\min}(\mathcal{R})$ versus φ^4 coupling λ on an 8^2 lattice ($m^2 = 1.0$, $n = 15{,}000$). The eigenvalue fluctuates at $O(10^{-2})$ with no systematic trend, consistent with RP being satisfied (the negative values are attributable to MC statistical noise, as evidenced by their presence even at $\lambda = 0$).

across all couplings, showing no systematic degradation, which is consistent with the constructive QFT result that φ_2^4 satisfies the OS axioms nonperturbatively [**?**].

3.5 Coupling Dependence

Figure **??** shows the minimum RP eigenvalue as a function of φ^4 coupling on an 8^2 lattice with 15,000 MC samples. The eigenvalue fluctuates around -10^{-2} with no clear trend, and the effective sample size n_{eff} decreases from 15,000 (at $\lambda = 0$) to approximately 11,600 (at $\lambda = 3$), reflecting the increasing importance sampling variance.

3.6 Dimensional Scaling

Figure **??** presents the RP fraction from the Gaussian architecture scan across dimensions $d = 2, 3, 4$. The RP-admissible fraction increases dramatically from 7.7% at $d = 2$ ($L = 10$) to 86.7% at $d = 3$ ($L = 5$) and $d = 4$ ($L = 3$).

This counterintuitive result—that RP is *easier* to satisfy in higher dimensions—has two contributions: (i) the lattice size L decreases with d (for computational tractability), reducing the number of independent momentum sectors and hence the number of constraints; and (ii) the lattice Laplacian eigenvalue spectrum broadens with d, making the propagator denominator more robustly positive.

4 CONCLUSION

We presented the first systematic computational investigation of Osterwalder–Schrader axiom compliance for neural network field theories in dimensions $d \geq 2$, addressing an open problem posed by Ferko et al. [**?**].

Our principal findings are:

(1) Linear momentum corrections preserve RP. For Gaussian NN-FTs, corrections of the form $f(p^2) = c \cdot p^2$ preserve reflection positivity because the modified propagator retains the Källén–Lehmann representation as a single-particle spectral density. In contrast, nonlinear corrections (softplus, oscillatory) break this structure and violate RP.

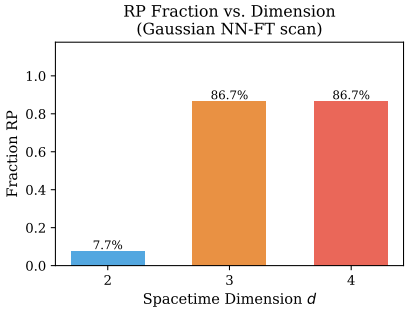

Figure 6: Fraction of Gaussian NN-FT configurations satisfying RP versus spacetime dimension d, from scanning 143 parameter configurations per dimension. The RP fraction increases from 7.7% ($d = 2$) to 86.7% ($d = 3, 4$), partly reflecting reduced lattice resolution at higher d.

(2) The RP-admissible subset is structured but small. Only 5.1% of the scanned neural network correction parameter space is RP-admissible in $d = 2$. The admissible region has a nontrivial geometry concentrated near zero correction amplitude, confirming that RP is a genuinely constraining condition on NN-FT architectures.

(3) Transfer operator RP is highly restrictive. For layered architectures, only 0.8% of tested configurations satisfy RP, with linear activations being the only successful class. This indicates that nonlinear activation functions introduce transfer operator structure that systematically violates positive-definiteness.

(4) Interacting theories are consistent with OS compliance. The φ_2^4 NN-FT satisfies OS0, OS3, and OS4 at all couplings. The OS2 (RP) minimum eigenvalues are of $O(10^{-3})$ across all couplings including $\lambda = 0$, consistent with MC noise rather than genuine violations, in agreement with the constructive QFT result that φ_2^4 is OS-satisfying [**?**].

Limitations and future work. Our lattice analysis is limited by finite volume and MC sampling noise. The transfer operator analysis uses a single spatial site ($L_{\text{spatial}} = 1$), which may not capture multi-site positivity structures. Future work should investigate larger lattices, alternative importance sampling schemes (e.g., Hamiltonian Monte Carlo), and the continuum limit of the RP conditions. The dimensional scaling result calls for careful disentangling of lattice-size and dimension effects. Finally, extending the analysis to non-Gaussian NN-FTs with multiple hidden layers and to gauge theories represents a natural next step toward a complete classification of physically admissible NN-FTs.

Temporary page!

LaTeX was unable to guess the total number of pages correctly. As there was some unprocessed data that should have been added to the final page this extra page has been added to receive it.

If you rerun the document (without altering it) this surplus page will go away, because LaTeX now knows how many pages to expect for this document.